Computer Simulations of Geodynamo and Mantle Convection

Project Representative
Akira Kageyama The Earth Simulator Center, Japan Agency for Marine-Earth Science and Technology

Authors
Akira Kageyama *1, Masanori Kameyama *1, Masaki Yoshida *1 and Mamoru Hyodo *1
*1 The Earth Simulator Center, Japan Agency for Marine-Earth Science and Technology

We have developed a new geodynamo simulation code based on the Yin-Yang grid in a spherical shell geometry. It is confirmed that the Yin-Yang grid suits well with massively parallel calculations. The sustained performance is 46% on 4096 processors of the Earth Simulator. The Yin-Yang grid has been also applied to the spherical mantle convection simulation in which effects of internal heating and strongly temperature-dependent viscosity on the global convection pattern are investigated. We have also improved our original algorithm "ACuTE" for mantle convection simulations and implemented it in a parallel code on the Earth simulator. By the ACuTE mantle convection code, the spatial variation of the thermal conductivity on the convective planforms in the box mantle convection is investigated.

Keywords: geodynamo, mantle convection, ACuTE method, Yin-Yang grid, multigrid method.

1. Development of High Performance Geodynamo Simulation Code by Yin-Yang Grid

Recently, we proposed a new grid system for the spherical geometry [5, 3] named "Yin-Yang grid" that is shown in Fig. 1. The Yin-Yang grid is a kind of overset grids [1]. Compared with other possible spherical overset grids, the Yin-Yang grid is simple in its configuration and metrics. Therefore the implemented code is compact. A family of Yin-Yang grids is constructed by a special kind of spherical dissections that divides a sphere into two identical pieces[2].

We have developed a geodynamo simulation code based on the Yin-Yang grid (Fig. 2). In this code, we apply the vectorization in the radial dimension of the three-dimensional arrays for physical variables in the magnetohydrodynamic (MHD) equations. The radial grid size is 255 or 511. We adopt the so-called "flat-MPI" approach, in which MPI is used both for the inter-node (distributed memory) and for the intra-node (shared memory) parallel processing. We first divide the whole computational domain into two identical parts or panels that correspond to the Yin grid's domain and the Yang grid's domain shown in Fig. 1(a). In our Yin-Yang geodynamo code, `MPI_COMM_SPLIT` is called to split the whole processes into two groups. (The total number of processes is even.) The world communicator is stored in a variable named `gRunner%world%communicator`, where `gRunner` is a nested derived type. For further parallelization within each component grid, we applied a two-dimensional decomposition in the horizontal space, colatitude θ and longitude ϕ. For this

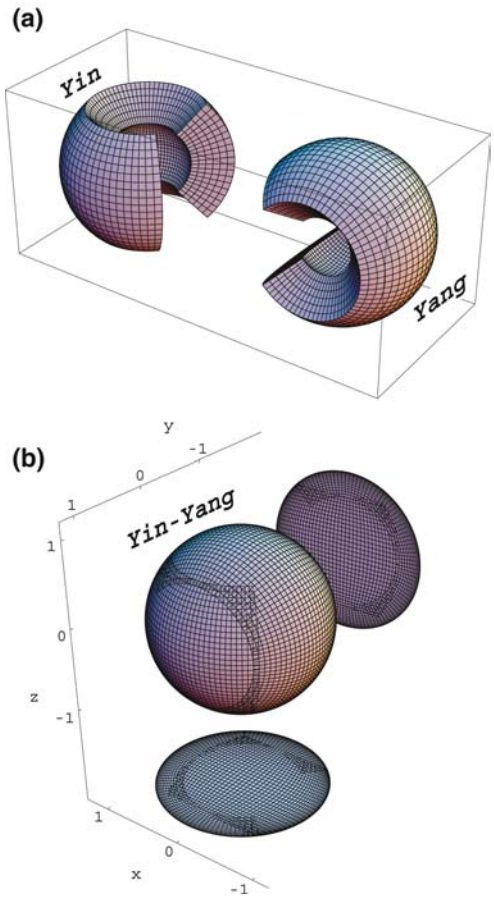

Fig. 1 Basic Yin-Yang grid. The Yin grid and Yang grid are combined to cover a spherical surface with partial overlap .

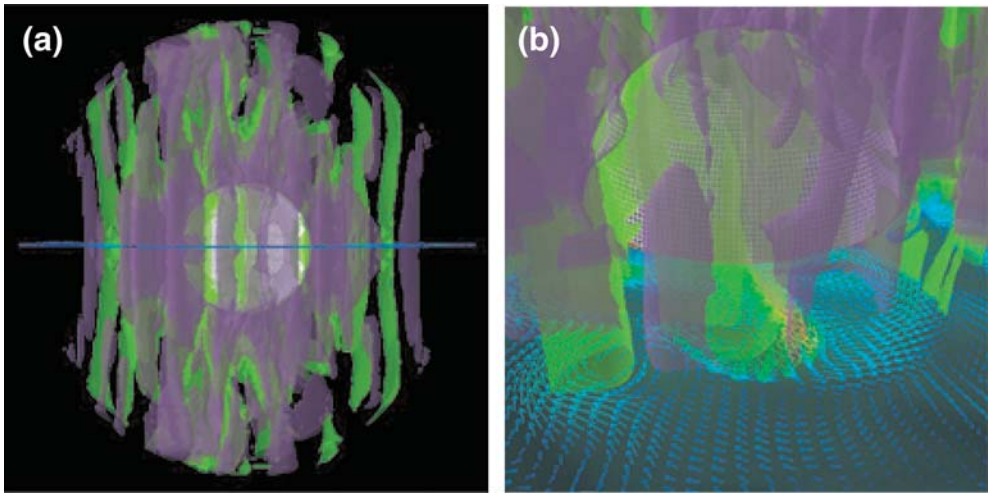

Fig. 2 Magnetohydrodynamic thermal convection structure obtained by 3888 processor calculation of Yin-Yang geodynamo code on the Earth Simulator. The total grid size is 255 (radial) × 514 (latitudinal) × 1538 (longitudinal) × 2 (Yin and Yang). In this visualization, grid points are reduced by a factor of 1/100. (a) Columnar convection cells viewed in the equatorial plane. Two colors indicate cyclonic and anti-cyclonic convection columns; (b) Same data with closer view.

purpose, we call `MPI_CART_CREATE` to make a two-dimensional process array with optimized rank order. For the intra-panel communication, `MPI_SEND` and `MPI_IRECV` are called between nearest neighbor processes. Each process has four neighbors (north, east, south, and west). The rank numbers for the neighbors, obtained by invoking `MPI_CART_SHIFT` with the panel's communicator `gRunner%panel%communicator`, are also stored in `gRunner`. Communication between two groups (Yin and Yang) is required for the overset interpolation. This communication is implemented by `MPI_SEND` and `MPI_IRECV` under `gRunner%world%communicator`.

The best performance of our Yin-Yang geodynamo code with this flat MPI parallelization is 15.2 Tflops [4], achieved by 4096 processors (512 nodes) with the total grid size of 511(radial) × times 514(latitudinal) × 1538(longitudinal) × 2(Yin and Yang). Since the theoretical peak performance of 4096 processors is 32.8 Tflops, this represents 46% of peak performance in this case. The high performance of the Yin-Yang geodynamo code is a direct consequence of the simple and symmetric configuration design of the Yin-Yang grid. For geodynamo study, it is necessary to follow the time development of the MHD system until the thermal convection flow and the dynamo-generated magnetic field are both sufficiently developed and saturated. (Initially, both the convection energy and the magnetic energy are negligibly small.) For the case of grid size of $255 \times 514 \times 1538 \times 2 = 4 \times 10^8$ with 3888 processes, it took six hours of wall clock time until both the dynamo-generated magnetic field and convection flow energy reached to a saturated, and balanced, level.

2. Development and Optimization of Algorithm for the Mantle Convection

The major difficulty in numerical simulations of mantle convection comes from the extreme rheological properties of mantle materials. In particular, the computation of the flow field is very time-consuming, where the velocity and pressure fields are simultaneously calculated from ill-conditioned elliptic differential equations at every timestep. In order to promote the large-scale numerical studies on mantle convection, we had proposed a new algorithm, hereafter called "ACuTE", for solving the flow field of mantle convection problems [7]. This algorithm iteratively solves the equations for conservation of mass and momentum for highly viscous and incompressible fluids together with the multigrid method. We had also developed a convection model in a three-dimensional rectangular domain. In FY2003 we obtained a moderate computational efficiency using 720 × 720 × 320 mesh divisions and 15 processor nodes (PNs) of the Earth Simulator.

In FY2004, we conducted a further optimization of the ACuTE algorithm in order to enhance the parallelization [6]. In particular, we improved the parallelization efficiency of multigrid procedures by a so-called "agglomeration" technique [10]. As summarized in Figure 3, we apply different patterns of domain decompositions depending on grid levels. On fine grid levels, the entire computational domain is decomposed into subdomains, which are assigned to different processor elements (PEs). On coarse levels, in contrast, we give up decomposing the entire meshes into subdomains, and assign the entire computations to one PE while leaving other PEs idle. A major benefit of the agglomeration is that no communication is required on grid levels where only one PE is

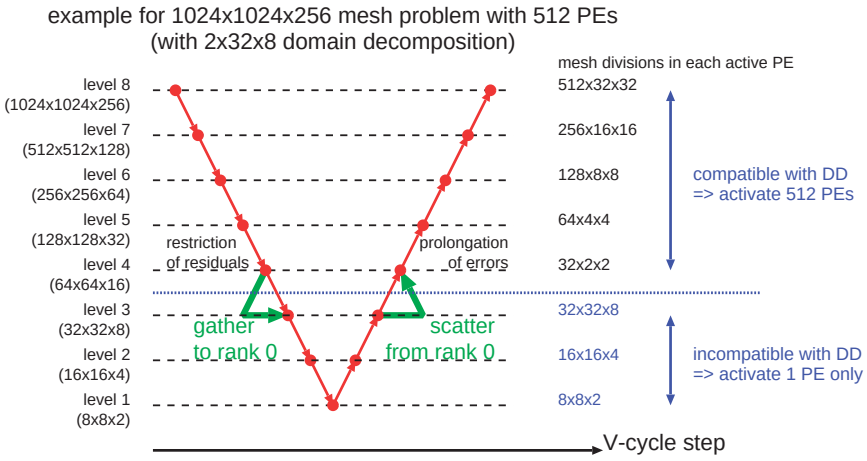

Fig. 3 A schematic diagram of the pattern of domain decompositions together with the course of the standard V-cycle of multigrid iterations. The dotted blue line indicates a threshold grid level which divides the entire grid levels into two groups. The grid levels finer than the threshold contain a sufficient number of meshes compared to that of available processor elements (PEs) for parallel computations, while the coarser levels do not. The calculations on the finer grid levels are performed in parallel using all available PEs, while the calculations on the coarser levels are done using only one PE with rank 0.

involved in computations. By this adaptation of multigrid procedures, we obtained sufficient vector and parallel efficiency using up to 64 PNs for the calculations with $1024 \times 1024 \times 256$ mesh divisions, and achieved 18% of peak performance.

3. Studies on the Influence of Variable Thermal Conductivity and Strongly Temperature-Dependent Viscosity on the Convective Planforms in the Mantle

The physical properties of mantle materials can vary owing to the ambient conditions such as temperature and pressure. For example, the viscosity of mantle minerals varies by several orders of magnitude mainly because of the temperature change. Much effort has been devoted so far to the effect of strong viscosity variation on convective planforms. On the other hand, it is also acknowledged that the thermal conductivity varies approximately by a factor of 10 within the mantle. The effect of its spatial variation, although modest, has been drawing the attention of the mantle convection researchers. In particular, some of recent works pointed out the importance of the radiative contribution of thermal conduction, which may be significant for high temperature.

Here we study the effect of the spatial variation in thermal conductivity k on the convective planforms in the mantle. A time-dependent convection in a rectangular box of 3000 km height and aspect ratio $6 \times 6 \times 1$ is considered. We employed an extended Boussinesq approximation, where the effects of adiabatic and viscous heating are included. The viscosity of mantle materials is assumed to be dependent on temperature T and depth. We take into account the temperature-dependence of thermal conductivity k, which mimics the effects of radiative heat transfer expected to be dominant in a hotter part of the mantle. In FY2004 we carried out several preliminary calculations using spatial mesh divisions of $512 \times 512 \times 128$. Figure 4 shows the snapshots of the upwelling regions obtained for the cases with (a) constant and (b) temperature-dependent thermal conductivity k. When k is constant (Figure 4a), the overall convection is characterized by major upwelling plumes at the center and the four corners of the domain, and is superimposed by several minor plumes ascending from the bottom surface due to the boundary-layer instability. When k depends on temperature T (Figure 4b), in contrast, the major upwelling occurs only at the center of the domain, and the instability is suppressed along the bottom surface. Our preliminary calculations suggest that under certain conditions the modest variation in thermal conductivity can exert significant impact on convective flow patterns, by stabilizing the boundary-layer instability at the bottom surface and by enlarging horizontal spacings of upwelling plumes. These results may imply the potential importance of the radiative heat transfer on the occurrence of “superplumes” observed in the Earth’s mantle.

4. Effects of Internal Heating on the Spherical Mantle Convection

Most of the heat for Earth’s mantle comes from the mantle itself, from a combination of radioactive decay of the heat-producing isotopes and secular cooling of the mantle. We have studied the effects of internal heating on the mantle convection heated from the bottom of the three-dimensional spherical shell. A Yin-Yang grid is used for the spatial discretization of basic equations governing the Boussinesq fluid

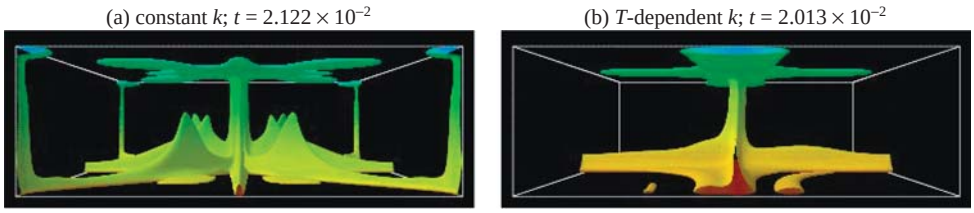

Fig. 4 Isosurfaces of the deviation of nondimensional temperature from its horizontal average $\delta T \equiv T - < T > = 0.05$ in a subdomain of $3 \times 3 \times 1$ for the cases where the thermal conductivity k is (a) constant and (b) dependent on temperature T.

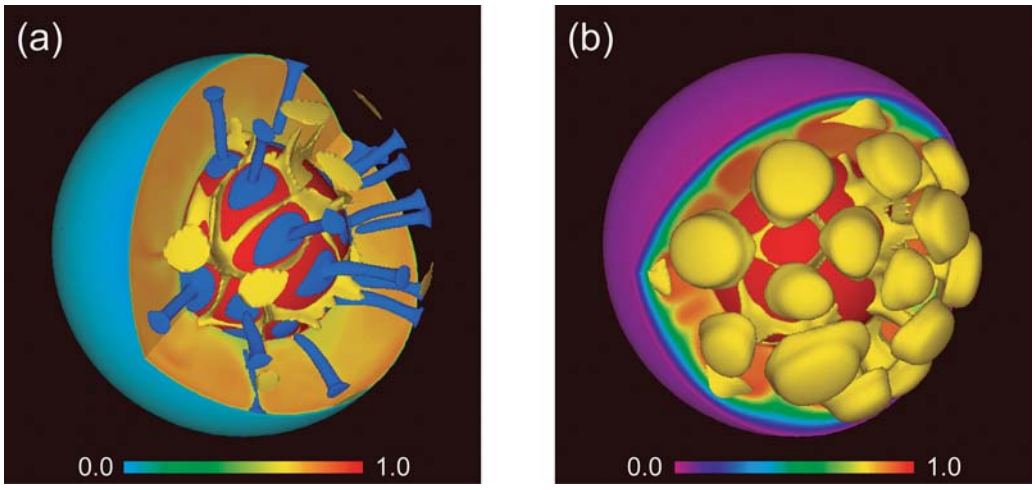

Fig. 5 Snapshots of the temperature field for the cases (a) with internal heating $H = 20$ and (b) strongly temperature dependent viscosity $\gamma_\eta = 10^6$. Non-dimensional temperatures range from 0 (cold) to 1 (hot) as indicated by color bars. The isosurfaces of temperature anomaly (the deviation from the horizontally averaged temperature at each depth) show (a) –0.1 (blue) and +0.1 (yellow), and (b) +0.03 (yellow).

convection [12]. The Rayleigh number defined by the bottom temperature T_{bot} is fixed at $Ra_{bot} = 10^7$, which is characteristic of the mantles of the terrestrial planets. Without internal heating, the thermal structure is strongly time-dependent, driven by narrow, cylindrical upwelling (hot) plumes surrounding by a network of long downwelling (cold) sheets. This feature is in contrast with the convective feature at low Rayleigh number ($Ra_{bot} < 10^5$) where the convection is nearly steady state [12]. The non-dimensional internal heating rate is here defined by $H \equiv \hat{H}\hat{d}^2 / \hat{\kappa}\hat{c_p}\Delta\hat{T}$, where $\hat{H}$ is the internal heating rate per unit mass, $\hat{d}$ the thickness of the mantle, $\hat{\kappa}$ the thermal diffusivity, $\hat{c_p}$ the specific heat at constant pressure, and $\Delta\hat{T}$ is the temperature difference of the mantle [11] An end-member case where H = 20 is shown in Figure 5a. As H is increased, the convective feature is dominated by the short-wavelength structure with numerous quasi-cylindrical downwellingsspaced relatively close together. The downwellings are surrounded by broad and diffuse upwellings of hotter fluid. Internal heating influences on the scale of convection pattern, especially on the shape of downwellings; a sheet-like feature is taken over by a cylindrical feature as the internal heating rate is increased.

5. Effects of temperature-dependent viscosity contrast

By the laboratory experiments on silicate rock deformation, the viscosity of the mantle rheology depends on the various parameters such as temperature, pressure and stress, and so on. Among them the temperature dependence has the strongest effect on the viscosity [11]. The effects of the temperature-dependent viscosity on mantle convection have, however, not been systematically studied by the use of three-dimensional spherical shell geometry. With our Yin-Yang grid code, we have performed calculations of the convection with the temperature-dependent viscosity when $Ra_{bot} = 10^6 - 10^7$. Internal heating of the mantle is not taken into account. The viscosity is here simply defined by $\eta = \exp\{-E(T - T_{bot})\}$ where E is the non-dimensional activation parameter, and T is the temperature. The viscosity contrast across the spherical shell is therefore defined by $\gamma_\eta \equiv \exp(E)$. Our results basically support the previous results [8]. As γ_η is increased, the convecting pattern is classified into the “mobile-lid” regime, the “sluggish-lid” regime, and the “stagnant-lid” regime, all defined by the previous two-dimensional study [9]. The moderate viscosity contrast ($\gamma_\eta = 10^3 - 10^4$) makes the convecting pattern long-wavelength structures, i.e., the sluggish-lid regime. Our pre-

vious study have shown that, at $Ra_{bot} = 10^6$, the convection pattern comes to be dominated by the degree-two pattern; the two-cell structure is formed that consists of one sheet-like downwelling and two cylindrical upwelling plumes [12]. In contrast, at $Ra_{bot} = 10^7$, the convection pattern comes to be dominated by the degree-one pattern; the one-cell structure that consists of a pair of cylindrical downwelling plume and cylindrical upwelling plume is formed. This finding indicates that the convecting feature on the sluggish-lid regime strongly depends on the Rayleigh number, although their symmetric patterns remain unchanged. The convective flow pattern that belongs to the stagnant-lid regime emerges when $\gamma_\eta \geq 10^5$. The characteristic thermal structure has a short-length scale comparable to the thickness of the mantle. The convection under the lid is characterized by numerous, small-scale cylindrical plumes surrounded by sheet-like downwellings (Figure 5b). The convective flow becomes weakly time-dependent; upwelling plumes are moving slowly in horizontal directions. This convective feature may be caused by the Rayleigh-Talor instability at the base of stagnant-lid. At $\gamma_\eta \geq 10^6$, the connected network of sheet-like downwelling reaches the middle to the bottom of the convecting layer. When γ_η is further increased ($\gamma_\eta \geq 10^8$), this sheet-like downwelling underneath a rather thick stagnant-lid completely reaches the bottom boundary of the mantle, so that we clearly observe large, mushroom-shaped upwelling plumes to develop the well-arranged convecting cells. The strongly temperature-dependent viscosity is necessary to reproduce the stagnant-lid that corresponds to the cold, stiff lithosphere on the terrestrial planets.

6. Summary

By FY2004, we had devised two numerical methods for simulations of the Earth's interior; (a) Yin-Yang grid, and (b) ACuTE algorithm. The Yin-Yang grid is a new spherical grid system that can be useful for a broad range of numerical problems in the spherical geometry. The ACuTE algorithm enables us to perform efficient and high-speed computations of the mantle convection problems. In FY2004, we first refined these two methods with a special emphasis on the parallel computation on the multiple nodes of the Earth Simulator. These improvements are implemented in the following three simulation programs developed in this fiscal year: (i) Yin-Yang geodynamo simulation code (spherical shell geometry, highly parallelized), (ii) Yin-Yang mantle convection code (spherical shell geometry, partially parallelized), and (iii) ACuTE mantle convection code (box geometry, highly parallelized). Running these codes on the Earth Simulator, we investigated various aspects of the dynamics of the core and mantle, including (1) magnetohydrodynamic convection and the geodynamo process in the core under low diffusion rates, (2) changes of the global patterns in the spherical mantle convection due to the internal heating and the strongly temperature-dependent viscosity, and (3) effects of the spatial variation in thermal conductivity on the convective planforms in the box mantle convection.

References

[1] G. Chesshire and W. D. Henshaw. Composite overlapping meshes for the solution of partial differential equations. *J. Comput. Phys*., 90 : 1 – 64, 1990.

[2] A. Kageyama. Dissection of a sphere and Yin-Yang grids. *J. Earth Simulator*, 3, 2005.

[3] A. Kageyama. Yin-Yang grid and geodynamo simulation. *Computational Fluid and Solid Mechanics*, Elsevier, 2005, 688 – 692.

[4] A. Kageyama, M. Kameyama, S. Fujihara, M. Yoshida, M. Hyodo, and Y. Tsuda. A 15.2 tflops simulation of geodynamo on the earth simulator. In *Proc. ACM/IEEE Supercomputing Conference 2004, SC2004*, Pitssburgh, PA, USA, November 2004.

[5] A. Kageyama and T. Sato. The 'Yin-Yang Grid': An overset grid in spherical geometry. Geochem. Geophys. Geosyst., 5(9) : 1 – 15, 2004.

[6] M. Kameyama. ACuTEMan: A multigrid-based mantle convection simulation code and its optimization to the Earth Simulator. *J. Earth Simulator*, 2005.

[7] M. Kameyama, A. Kageyama, and T. Sato. Multigrid iterative algorithm using pseudo-compressibility for three-dimensional mantle convection with strongly variable viscosity. *J. Comput. Phys*., 206(1) : 162 – 181, 2005.

[8] J. T. Ratcliff, P. J. Tackley, G. Schubert, and A. Zebib. Transitions in thermal convection with strongly variable viscosity. *Phys. Earth Planet. Inter*, 102 : 201 – 212, 1997.

[9] S. Solomatov. Scaling of temperature- and stress-dependent viscosity convection. *Phys. Fluids*, 7 : 266 – 274, 1995.

[10] U. Trottenberg, C. Oosterlee, and A. Schüller. *Multigrid*. Academic Press, 2001.

[11] D. L. Turcotte and G. Schubert. *Geodynamics*. Cambridge Univ. Press, 2002.

[12] M. Yoshida and A. Kageyama. Application of the Yin-Yang grid to a thermal convection of a Boussinesq fluid with infinite Prandtl number in a three-dimensional spherical shell. *Geophys. Res. Lett*., 31(12), 2004.

地球ダイナモとマントル対流のシミュレーション

プロジェクト責任者
陰山　聡　地球シミュレータセンター，海洋研究開発機構
著者
陰山　聡*1，亀山　真典*1，吉田　晶樹*1，兵藤　守*1
*1　地球シミュレータセンター，海洋研究開発機構

我々は、地球シミュレータ(ES)を駆使した大規模計算機シミュレーションを通じて、地球ダイナモとマントル対流のダイナミクスを理解することを目指している。そしてそのために必要となる大規模並列計算手法や基本アルゴリズムの開発にも積極的に取り組んでいる。本年度はまず、我々が独自に考案した新しい球面格子「インヤン格子」をコア対流、つまり地球ダイナモのシミュレーションプログラムに適用し、その並列化とチューニングを行った。その結果、ESの512ノードを使った計算で、ピーク性能の46％の演算性能を記録することができた。これは、インヤン格子が大規模な並列計算にも適した優れた計算格子であることを証明するものである。また今年度開発したこのコードによって、従来の地磁気ダイナモシミュレーションと比較して、より現実的なダイナモ過程を研究することが可能となった。従来のシミュレーションよりも高解像度で大規模な計算、つまり低い散逸係数のもとでの計算が可能となったためである。

また我々は、インヤン格子を球殻マントル対流シミュレーションコードにも応用している。このコードは昨年度に引き続いて開発しているものである。今年度は、マントル物質の内部発熱と、粘性率の強い温度依存性、の二つが対流パターンにどのような影響を与えるかについて調べた。本年度の研究から、粘性率の温度依存性の強弱によってマントル対流のパターンは、(a) mobile-lid領域、(b) sluggish-lid領域、(c) stagnant-lid領域、の3つに分類できることが分かった。また、粘性率の温度依存性がそれほど強くない場合(sluggish-lid領域)では、レーリー数が上がるにつれて、二つの上昇流をもつ対流パターンから、一つの上昇流をもつ対流パターンに遷移することが見いだされた。粘性率の温度依存性が強いstagnant-lid領域では、短い長さスケールを持つ多数の対流構造が特徴的となる。粘性率の温度依存性をさらに強めると、マッシュルーム型の上昇プルームが規則的に並び、対流層の上端には比較的厚くて固いstagnant-lidが形成される。これは地球型惑星の表面に見られるリソスフェアに対応するものと考えられる。

また今年度は、マントル対流の高速シミュレーションを実現するために我々が開発した独自のアルゴリズムACuTE法の改良にも取り組んだ。改良のポイントは、ACuTE法で行っている多重格子法の計算効率の改善である。多重格子法では、格子レベルが低く(粗く)なるにつれて計算規模が小さくなるために、ベクトル化効率と並列化効率が低下する。このために我々はagglomerationと呼ばれる手法を導入した。agglomerationでは、ある格子レベル以下の計算は一つのプロセッサに計算を集中させる。これにより我々は$1024 \times 1024 \times 256$格子の箱形マントル対流計算において、地球シミュレータの64ノードでピーク性能の18%という、マントル対流では世界最高レベルの性能を実現することができた。そして、この改良を取り込んだ箱型領域のACuTEマントル対流計算により、今年度は特に熱伝導率の温度依存性が対流形態に与える影響を詳細に調べた。熱伝導率が空間的に一様な場合と、温度依存性がある場合のシミュレーション結果を比較したところ、熱伝導率の温度依存性があると、マントル対流の上昇プルームの数が少なくなることがわかった。この結果は、現実の地球のマントル対流にある大きなスケールのプルーム(スーパープルーム)の発生に熱伝導率の温度依存性が関与している可能性を示唆するものである。

キーワード：地球ダイナモ，マントル対流，ACuTE法，インヤン格子，多重格子法